Phenomenological description of ion-beam-induced epitaxial crystallization of amorphous silicon

Francesco Priolo
Dipartimento di Fisica, Università degli Studi di Catania, corso Italia 57, I-95129 Catania, Italy

Corrado Spinella
Istituto di Metodologie e Tecnologie per la Microelettronica del Consiglio Nazionale delle Ricerche, I-95100 Catania, Italy

Emanuele Rimini
Dipartimento di Fisica, Università degli Studi di Catania, corso Italia 57, I-95129 Catania, Italy
(Received 27 September 1989)

In this paper we report detailed experimental measurements on the dependence of the ion-beam-induced epitaxial crystallization (IBIEC) of amorphous silicon on dopant concentration. The results show that the presence of B, P, and As dopants enhances IBIEC. In particular a logarithmic relationship between the ion-induced growth rate and dopant concentration is found for all of the impurities. In order to explain this behavior a phenomenological model of IBIEC will also be presented. The model postulates that the same defect is responsible for both thermal and ion-beam annealing. It combines the structural and electronic features of the description proposed by Williams and Elliman for conventional thermal epitaxial growth, with the intracascade approach of Jackson to the ion-assisted regrowth. Defects responsible for IBIEC are identified in kinklike steps formed onto [110] ledges at the crystalline-amorphous interface. These kinks are assumed to be generated thermally within the thermal-spike regime of each collision cascade. After defect generation, then, our approach follows Jackson's as far as the temporal evolution of defects is concerned. The model can account for all of the experimental results previously explained by the Jackson model and, moreover, can account for the doping and orientation dependences of IBIEC. This description is discussed and quantitatively compared with the experimental data.

I. INTRODUCTION

Ion-beam irradiation of semiconductors represents a field of active research for both its basic aspects and its technological applications. Recently the ion-beam-induced epitaxial crystallization (IBIEC) of amorphous Si (*a*-Si) has raised several fundamental questions on the processes governing the nonequilibrium phase transitions produced by ion irradiation.[1–8]

The transition from the amorphous to the crystalline phase in Si can be obtained at temperatures as low as 200 °C by irradiating the sample with an energetic ion beam. The impinging ions should have a range greater than the original crystalline-amorphous (*c-a*) interface; on penetrating into the sample, they generate point defects which provide atomic mobility for a planar layer-by-layer crystallization. IBIEC has a relatively weak temperature dependence, being characterized by an apparent activation energy of ~ 0.3 eV.[3,5,6] The dependences on crystal orientation and on impurities dissolved in the amorphous layer are weak too: the growth rate along the $\langle 111 \rangle$ orientation is 2–4 times slower than along the $\langle 100 \rangle$ orientation,[9–11] a dopant concentration of $1 \times 10^{20}/\text{cm}^3$ enhances the rate by a factor of 2–3,[6,9] and a simultaneous B and P doping, at the same concentration, produces a partial compensation, being the growth rate smaller than that of a simply B-doped layer, but still higher than that of intrinsic material.[6] Moreover the opposite process, i.e., a layer-by-layer amorphization from a preexisting *c-a* interface, has been observed by decreasing the irradiation temperature or by increasing the dose rate.[8]

These data should be contrasted with conventional thermal annealing[12] where (i) and epitaxial crystallization occurs only for temperatures > 500 °C, (ii) the activation energy is 2.7 eV, (iii) the rate along $\langle 111 \rangle$ orientation is ~ 25 times slower than along $\langle 100 \rangle$ orientation, (iv) dopants can enhance the rate by almost 2 orders of magnitude, (v) simultaneous *p*- and *n*-type doping produces a compensating effect on the growth rate which reduces to that of intrinsic *a*-Si.

A few attempts[13–15] have been made to explain IBIEC by means of phenomenological models. In particular Atwater and co-workers[13,14] have described the process in terms of an irradiation-dependent chemical potential. According to this description, planar amorphization occurs when the free energy of the damaged crystal exceeds that of the irradiated amorphous region. Alternatively, Jackson[15] has proposed an intracascade model where each impinging ion converts a small volume of crystal at the *c-a* interface to the amorphous state and, at the same time, creates defects that promote crystallization. The model is based on the assumptions that defects of a single kind are responsible for IBIEC and that these defects annihilate in pairs. It is quite striking that the Jackson model can account for so much of the experi-

mental data. The model fits the temperature and flux dependences of both crystallization and amorphization,[8] the frequency dependence of the growth rate in pulsing experiments,[16] and the transition from the IBIEC regime to the thermal regime.

The Jackson model represents undoubtedly a fascinating description of IBIEC, nevertheless, several fundamental questions are still to be answered. They deal mainly with the microscopic structure of the generated defects and with the mechanism of generation within the collision cascade. Moreover, experimental data such as the dependences of IBIEC on substrate orientation and on dopants dissolved in the amorphous layer are still not understood at all. We think that the presence of these dependences represents an important hint for a complete understanding of IBIEC. Our opinion is based on the observation that these effects are similar to those observed during pure thermal annealing (with the exception of the compensation effect). The presence of similar effects suggests that similar processes should be operative in the two cases.

In this paper we propose a phenomenological model of IBIEC in which the thermal-spike regime, within a single collision cascade, plays the dominant role in the production of defects responsible for the crystallization. Our description combines the approach of the model proposed by Jackson[15] with the structural and electronic features of the models proposed for conventional thermal regrowth.[17–19] In the following we will first present some detailed experimental measurements on the dependence of IBIEC on dopant concentration, then we will introduce our thermal-spike description of IBIEC, and, finally, a quantitative comparison between the model and the experimental results will be reported.

II. EXPERIMENTAL PROCEDURE AND RESULTS

Though dopants are known to influence IBIEC,[6,9] no systematic quantitative study on the dependence of the ion-induced growth rate on dopant concentration has been carried out up to date. Such an experiment is reported in the following.

Preamorphized Si layers, ~160 nm thick, on ⟨100⟩-oriented Si substrates were implanted with B, P, and As at energies in the range 20–120 keV and at doses in the range 5×10^{14} to $1\times10^{16}/cm^2$. These implants produce almost Gaussian impurity profiles with peak concentrations ranging from 8×10^{19} to $2\times10^{21}/cm^3$ and lying at a depth of ~60–80 nm.

Samples were regrown by irradiation with a 600-keV Kr^{2+} beam electrostatically scanned over a 1 in. diam sample area. The ion flux was $1\times10^{12}/cm^2$ sec. During irradiations the samples were held onto a resistively heated copper block whose temperature was maintained constant at a value of 350±3 °C. In order to obtain a direct comparison with the doped layers, impurity-free *a*-Si layers were also regrown under identical conditions.

The ion-induced motion of the *c-a* interface was followed *in situ* by means of transient reflectivity measurements. This technique was firstly introduced by Olson *et al.*[20] to study the pure thermal regrowth and it has been recently applied also to IBIEC.[6] During Kr irradiation a 5-mW σ-polarized He-Ne laser ($\lambda=633$ nm) was focused onto the sample surface and the reflected light was detected by a photodiode connected with an *X-Y* recorder. As soon as the *c-a* interface advances towards the surface, the reflectivity changes due to successive constructive and destructive interferences between the light reflected from the surface and that reflected from the moving buried interface. For instance, an advancement of the *c-a* interface by 33 nm produces a transition, in the reflectivity signal, from a maximum to a consecutive minimum (or vice versa). A quantitative analysis of the experimental reflectivity signals directly yields the ion-induced growth rate as a function of depth.

Figure 1 reports the experimental reflectivity traces, for both an impurity-free (upper part) and a B-doped (lower part) *a*-Si sample, as a function of the irradiated Kr dose. In the latter case, B had been preimplanted in the sample at an energy of 20 keV and at a dose of $5\times10^{14}/cm^2$. Both signals present a series of oscillations with increasing the irradiation dose. This behavior indicates that the growth boundary is advancing in a planar fashion towards the surface. In particular the impurity-free amorphous layer is completely recrystallized after a Kr dose of $\sim1.1\times10^{16}/cm^2$, while the complete regrowth of the B-doped layer requires an irradiation dose of only $\sim6\times10^{15}/cm^2$ (as also confirmed by Rutherford backscattering spectrometry in combination with the channeling effect). The presence of B, therefore, strongly enhances the kinetics of the process.

IBIEC of *a*-Si layers with Gaussian impurity profiles allows us to measure, in a single run and in a wide range of values, the dependence of the growth rate on impurity concentration. This is shown in Fig. 2 where we report the ion-induced growth rates, deduced from an analysis of the reflectivity signals, versus the depth. Data for both the B-doped (solid line) and the impurity-free (dashed line) samples are shown. In the same figure the B profile is also reported in a logarithmic scale. The growth rate of the impurity-free sample slightly depends on depth. This is a well-known behavior and has been ascribed to

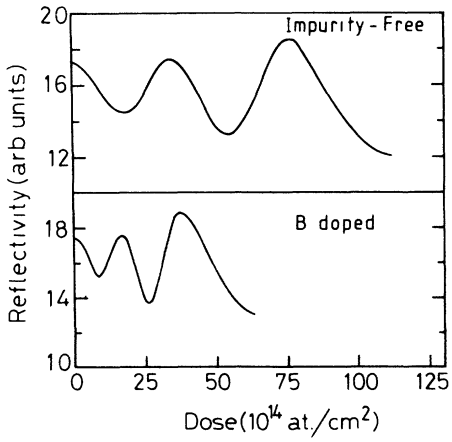

FIG. 1. Experimental reflectivity traces for an impurity-free (upper part) and a B-doped (lower part) *a*-Si layer recrystallized at 350°C by 600-keV Kr^{2+} irradiation as a function of the irradiation dose.

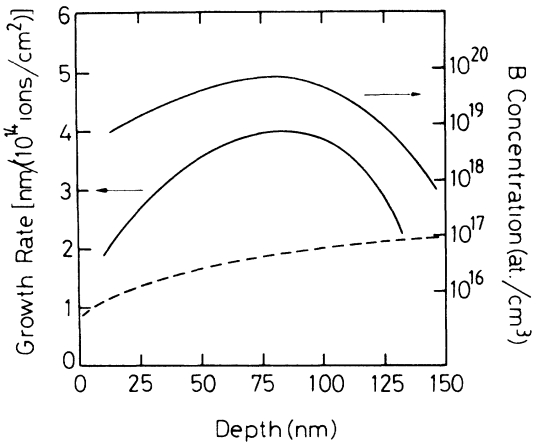

FIG. 2. Ion-induced growth rates vs depth as deduced from an analysis of the data shown in Fig. 1. Growth rates for both an impurity-free sample (dashed line) and a B-doped sample (solid line) are reported. The B profile is also reported in the figure in a logarithmic scale (right-hand side).

the depth dependence of the energy deposited into elastic collisions by the impinging Kr ions.[6] The growth rate of the B-doped layer is much higher with respect to that of the intrinsic material. For instance, at a B concentration of $8\times10^{19}/cm^3$ (corresponding to a depth of $\sim$80 nm) the rate is enhanced by more than a factor of 2. It should be noted that this very same B concentration would have produced an enhancement by a factor of 10 during pure thermal annealing.[12] The most interesting feature of Fig. 2, however, is the dependence on depth presented by the growth rate. The shape of the curve shows strong similarities with the B profile plotted in a logarithmic scale. This is quite intriguing behavior and suggests the presence of a logarithmic relationship between the ion-induced growth rate and the B concentration.

Experiments similar to those so far reported were also performed for P-doped and As-doped *a*-Si layers. In particular, recrystallization was induced on samples with peak dopant concentrations varying by more than 1 order of magnitude. The results are similar to those shown for the B-doped layers, though the rate enhancements are less pronounced. Moreover, the logarithmic dependence of the growth rate on dopant concentration also appears to be confirmed for these impurities.

The presence of a simple, well-defined functional form of the concentration dependence represents an important experimental result which any model wishing to explain IBIEC should be able to account for.

III. PHENOMENOLOGICAL APPROACH

Our phenomenological description of IBIEC is based on the simple observation that similar effects are present in both conventional and ion-beam annealing. In fact, in both cases dopants produce a rate enhancement, and in both cases the growth along ⟨100⟩ orientation is faster than that along ⟨111⟩ orientation. The presence of similar effects strongly supports the idea that the same defect is responsible for both thermal annealing and ion-induced regrowth.

Spaepen and Turnbull[17] have proposed a structural model of thermal annealing in which the *c-a* interface is resolved into a free-energy minimum by the formation of terraces with a {111} orientation. The regrowth proceeds then via a bond-breaking process and a subsequent rearrangement along the [110] edges which form on this terraced interface structure. Since the number of [110] ledges onto {111}-oriented terraces strongly depends on crystal orientation, this description is able to qualitatively explain the orientation dependence observed in conventional thermal annealing.

Williams and Elliman[19] have extended the structural concepts put forward by Spaepen and Turnbull. In their phenomenological model the *c-a* interface is assumed to present the same kind of terraced structure. Moreover, the defect (or "growth site") responsible for recrystallization is proposed to be a kink along a [110] ledge. Amorphous atoms at a kink site, unlike other atoms at the *c-a* interface, have at least two bonds with the crystalline phase. This position is therefore the most favorable for the occurrence of recrystallization which proceeds via a kink motion along the [110] ledges. A simplified representation of a (100) *c-a* interface, according to the description given by Williams and Elliman, is shown in Fig. 3. The {111} oriented terraces are clearly visible. Along [110] ledges (*AB*), which connect different terraces, kinks (*CD*) are formed. The motion of these kinks, indicated by the arrows, produces recrystallization. This model not only gives a microscopic description of thermal annealing, but also provides a qualitative understanding for the influence of dopants. In fact, since kinks exist in charged states, their number depends on the position of the Fermi level and, in turn, on dopant concentration.

Our description of IBIEC, in analogy with conventional thermal annealing, assumes that kinks at [110] ledges are the defects responsible for the process. This assumption contrasts with the currently accepted picture of

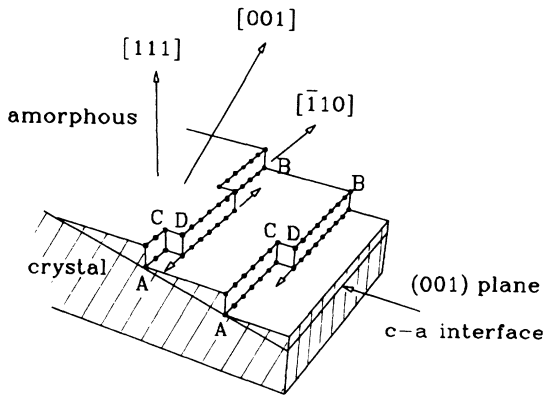

FIG. 3. Kinklike steps at a *c-a* interface according to the model of thermal crystallization proposed by Williams and Elliman (Ref. 18). The lower part of the figure (hatched) represents crystal, while the upper part is amorphous. The (001) *c-a* interface is composed by {111}-oriented terraces; along the [110] ledges (*AB*), present onto this terraced structure, kink steps (*CD*) form. The motion of these kinks (sketched by arrows) produces crystallization.

IBIEC, nevertheless, it seems quite reasonable.

It has been generally thought that defects promoting IBIEC are produced athermally by means of the elastic collisions experienced by the incoming ions. In particular these defects have been identified with vacancies[3,4,8] or with dangling bonds[15] according to the different descriptions. This picture is supported by the experimental observation that the ion-induced growth rate depends just on the energy deposited by the beam in elastic collisions,[4-6] while the energy deposited into electronic excitations plays no role. Accurate experiments of IBIEC in channeling conditions[5] have shown, however, that only those defects formed just at the *c-a* interface are responsible for the process, since the contribution of defects formed far from the interface (< 10 Å) is absolutely negligible. This important result is not clearly understood if IBIEC is ascribed to the previously mentioned defects. In fact, those defects can actually diffuse long distances far from the generation site and should be able to reach the interface (and contribute to IBIEC) also if generated elsewhere. The kinklike defect proposed in the present model, instead, is a structural deformation on the *c-a* interface; it does not exist away from it: it is generated there, diffuses there and annihilates there. If kinks are the defects responsible for IBIEC, then, the channeling experiment is automatically explained.

Unlike vacancies, kinks cannot be thought to be generated athermally by means of elastic collisions. Therefore, in our description of IBIEC, we assume further that kink generation occurs thermally within the thermal-spike regime of each collision cascade. This is a strong assumption but it does not seem unreasonable. In fact, following the collisional phase (which lasts $\sim 10^{-13}$ sec), a region of ~ 10 nm in diameter surrounding the ion track experiences a regime of quasiequilibrium in which the temperature is raised to several thousands of degrees. This thermal-spike regime lasts for several picoseconds and, due to the high temperatures, it should be possible to thermally generate a high kink density.

Recently, the dominant role played by the thermal-spike regime in other beam-induced effects, such as atomic mixing, has been pointed out by Diaz de la Rubia *et al.*,[21] who performed sophisticated molecular-dynamic simulations. Their calculations have demonstrated that the collisional phase is indeed followed by a local melting which persists for several picoseconds. The atomic mixing occurred mainly in this thermal regime rather than in the previous collisional phase. These results agree well with the experimental observation that the thermochemical parameters of materials strongly influence their mixing efficiencies.[22]

A thermal-spike description of IBIEC still maintains the dominant influence of elastic collisions in determining the growth rate. Radial ambipolar diffusion away from the ion track of the dense electron-hole plasma generated by ionizations occurs in a time scale of about 10^{-13} sec. The temperatures produced within the collision cascade are therefore independent of the energy deposited by the ions into electronic excitations.

We note further that kinks, like the defects required by the Jackson model[15] of IBIEC, create and annihilate in pairs. This is clearly illustrated in Fig. 4. The figure represents a section of the sample along a {111} terrace at the *c-a* interface. Crosses are crystalline atoms in the lower plane, while the solid circles are crystalline atoms in the upper plane. The [110] ledge onto a {111} terrace is clearly indicated in the figure. Figure 4(a) shows the nucleation of a couple of new kinks along a [110] ledge. The crystallization of the atom labeled *A* produces two kink sites in the positions labeled *B* and *C* (open circles). These are two amorphous atoms and each of them shares two bonds with crystalline atoms. The atoms *B* and *C* are the next to recrystallize. Regrowth will then proceed by a motion of these two kinks along the [110] ledge. The main issue, however, is that kinks form in pairs. Figure 4(b) shows the annihilation of two kinks. In this figure kinks *D* and *F* move in opposite directions, one against the other, on the same ledge. Recrystallization of atoms *D*, *F*, and finally of atom *E* will produce the annihilation of the two kinks. Therefore, kinks do annihilate in pairs. This demonstrates that kinks behave like the defects postulated in the Jackson model of IBIEC.

Our description of IBIEC then assumes that after kink generation, occurring at high temperatures in a time scale of $\sim 10^{-11}$ sec, their temporal evolution occurs in a time scale of $\sim 10^{-6}$ sec, at the low substrate temperature (200–300 °C), and is completely described by the Jackson model. The growth rate, within a good approximation, is then described by:[15]

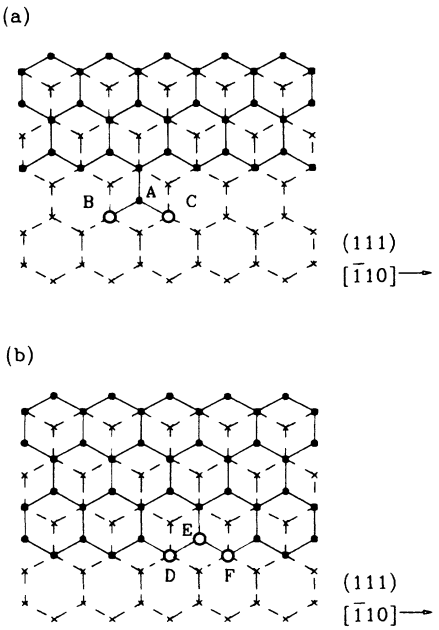

FIG. 4. A section of the *c-a* interface along a {111} terrace is represented. The crosses represent atoms in the lower plane, while the solid circles are atoms in the top plane. In (a) the recrystallization of the atom labeled *A* generates two kink sites (*B* and *C*). These are the next amorphous atoms to recrystallize. In (b) the two kinks labeled *D* and *F* are going to annihilate each other. Recrystallization of atoms *D*, *F*, and finally *E* will produce the annihilation. Therefore, kinks generate and annihilate in pairs.

$$R=\frac{dx}{d\phi}=\frac{a\langle N\rangle\Lambda}{\tau_j\dot{\phi}}-V_\alpha=\frac{\pi r_0^2\Lambda}{\sigma^2}\ln\left[\frac{\sigma^2 a\tau_0}{\tau_j}N_0\right]-V_\alpha\ , \tag{1}$$

where a is the lattice parameter, $\langle N\rangle$ is the temporal average defect density within a single collision cascade, Λ the volume crystallized in a single defect jump, τ_j is the jump period, V_α the volume amorphized by one ion, ϕ the irradiation dose, $\dot{\phi}$ the ion flux, r_0 the radius of the collision cascade, σ^2 is the cross section for defect annihilation, τ_0 the time between the arrival of two consecutive ions in the same region, and N_0 the defect density generated by one ion. The product aN_0 represents the number of defects per unit area generated at the *c-a* interface. In the present description, however, aN_0 is the areal density of kinks thermally generated within a single collision cascade.

A few observations are important. In the Jackson model 25 defect jumps are required to recrystallize an atom. In the present model, instead, a single kink jump results in the transition of one atom from the amorphous to the crystalline phase. This means that Λ equals an atomic volume. As a matter of fact, the fits performed by Jackson can be left almost unchanged by a simultaneous rescaling of both σ^2 and τ_j (which must be increased by a factor of 25). The numerical values of the parameters used in this work are reported in Table I. A second observation concerns the particular meaning assumed by V_α in this model. V_α is thought to be due to interstitials produced during direct collisions and which condense at the *c-a* interface. Of course the sites available for condensation in the amorphous phase at the interface are just the [110] ledges (see Figs. 3–4). The numerical value of V_α is therefore proposed to be orientation dependent. A third observation concerns the actual value of N_0. This value can be estimated by a fit of the experimental growth rate of a $\langle 100\rangle$ oriented impurity-free sample (see Fig. 2) with the use of Eq. (1). N_0 was found to be $\sim 4\times 10^{19}/\text{cm}^3$. The question arising at this point is whether this kink concentration can indeed be thermally generated within a single thermal spike. A rough estimate can be made by assuming a cylindrical spike[23] and calculating all the defects generated over the fast thermal transient. This has been done by integrating the following expression in a time interval in which the temperature is below 1700 K (the material should be solid to generate kinks):

TABLE I. Numerical values of the parameters used in this work.

Λ	σ^2	τ_j
cm^3	cm^2	sec[a]
2×10^{-23}	7.4×10^{-14}	3×10^{-5}
r_0	N_{0s}	τ_0
nm	cm^{-3}	sec[b]
7.2	5×10^{19}	0.6

[a]At 350°C.
[b]Value for a dose rate of 1×10^{12} ions/cm^2.

$$N=\frac{1}{\pi r_0^2}\int_0^{r_0}ds\,2\pi s\int_0^{\infty}dt\ A\exp\left[-\frac{E_T}{kT(s,t)}\right], \tag{2a}$$

where the variation of temperature with space and time is described by

$$T(s,t)=\frac{\varepsilon}{4\pi c\rho Dt}\exp\left[-\frac{s^2}{4Dt}\right]+T_{\text{sub}}\ . \tag{2b}$$

In these equations r_0 is the radius of the cylindrical collision cascade, A is the preexponential factor for defect generation, E_T the total activation energy of the process, ε the nuclear energy loss of the incident ion, c the heat capacity, ρ the density of the material, D the thermal-diffusion coefficient, and T_{sub} is the substrate temperature. The numerical values of these parameters can be taken from the Jackson model[15] and from the known thermal properties of Si.[24,25] A numerical integration of Eqs. (2a) and (2b) yields a value of $\sim 1\times 10^{19}/\text{cm}^3$. This number makes plausible the occurrence of a thermal kink generation within each collision cascade. Sophisticated molecular-dynamics simulations should be made to verify this point in more detail.

It should be noted that all of the experimental data accounted for by the Jackson model are still explained in the present approach. Moreover, our description can explain both the orientation and the doping dependences as discussed in the next section.

IV. DISCUSSION

A. Orientation dependence

Simple geometrical considerations show that the number of [110] ledges onto $\{111\}$-oriented terraces at the *c-a* interface is proportional to $\sin\theta$, θ being the angle between the $\langle 111\rangle$ axis and the surface normal. In a model in which defects annihilate in pairs, the steady-state defect concentration produced by a slow thermal process is proportional to the square root of the number of sites available for defect generation.[15] In the present approach, therefore, the thermal growth rate is proportional to the square root of $\sin\theta$, in qualitative agreement with the orientation dependence measured in pure thermal annealing.

Within the fast thermal-spike regime of a single collision cascade, kink annihilation is expected to be negligible and a steady-state defect population is never achieved. In this nonequilibrium case the generated kink population will be proportional to the number of generation sites and can therefore be expressed as $N_0=N_{0s}\sin\theta$. For instance, in the case of $\langle 100\rangle$-oriented Si, for which N_0 is known, θ equals 54.7°. N_{0s} is therefore equal to $\sim 5\times 10^{19}/\text{cm}^3$.

For orientations deviating from the $\langle 100\rangle$ direction, the growth rate can still be expressed by Eq. (1) provided that N_0 is calculated for the right θ value. In particular, neglecting V_α in Eq. (1) (which can be done in conditions far from the amorphization regime), the ratio between the ion-induced growth rate along $\langle 100\rangle$-oriented substrates ($R_{\langle 100\rangle}$) and that along substrates deviating by an angle θ

from the ⟨111⟩ orientation (R_θ), simply reduces to

$$\frac{R_{\langle 100\rangle}}{R_\theta}=1+\frac{\ln[\sin(54.7°)/\sin\theta]}{\ln[(\sigma^2 a\tau_0/\tau_j)N_{0s}\sin\theta]} . \quad (3)$$

For instance, for ⟨110⟩-oriented Si ($\theta=35.3°$), Eq. (3) yields a value of ~1.05. This agrees well with the experimental data in which no difference in the rate was observed between ⟨100⟩ and ⟨110⟩ orientations.[10].

In the case of ⟨111⟩-oriented Si this structural model would predict a zero growth rate for both thermal and ion-beam annealing. However, in order to explain conventional thermal annealing, Spaepen and Turnbull[17] have noted that only a slight misorientation from the exact ⟨111⟩ direction would produce enough [110] ledges to account for the finite value of the growth rate. In particular a value of $\theta=0.2°$ results in a thermal growth rate ~25 times smaller than that along ⟨100⟩ Si, in agreement with the experimental data. We have calculated the ratio between the ion-induced growth rate along ⟨100⟩ orientation and that along ⟨111⟩ orientation by using this value of θ in Eq. (3). The calculated ratio yields a value of 3.7. This value is in good agreement with the experimental results where the ion-induced growth rate on ⟨111⟩-oriented Si is reported to be between a factor of 2 and 4 (Refs. 9–11) smaller with respect to that onto ⟨111⟩-oriented Si.

B. Doping dependence

The influence of dopants on IBIEC is explained as well, provided that kinks, as supposed in thermal crystallization,[19] are allowed to exist in charged states. A dopant concentration N_d, changing the position of the Fermi level, will modify the number of generated kinks, N, according to

$$\frac{N}{N_0}=1+g\frac{fN_d}{N_c}\frac{1}{\tau_s}\int_0^{\tau_s}\exp\left[-\frac{E_d}{kT(t)}\right]dt , \quad (4)$$

where N_0 is the number of kinks generated in the absence of dopants, g is the degeneracy factor, f the fraction of electrically active dopants, N_c is the density of states in the conduction band, τ_s is the duration of the thermal spike, E_d is the donor level, k the Boltzmann constant, and T the temperature within the thermal spike. An analogous equation can be written for acceptors. The ion-induced growth rate of doped silicon will therefore be

$$R=\frac{\pi r_0^2\Lambda}{\sigma^2}\ln\left\{\frac{\sigma^2 a\tau_0}{\tau_j}N_0\left[1+g\frac{fN_d}{N_c}\frac{1}{\tau_s}\int_0^{\tau_s}\exp\left[-\frac{E_d}{kT(t)}\right]dt\right]\right\}-V_\alpha . \quad (5)$$

The presence of dopants, thus, produces a rate enhancement. The effect, however, is not very strong since the term corresponding to the doping enhancement is found within a logarithm. All of these observations are in qualitative agreement with the experimental results. In particular the difference between the growth rate of a doped sample and that of an undoped sample regrown under identical conditions will simply reduce to

$$R_{\rm diff}=\alpha\ln(1+\beta N_d) , \quad (6)$$

where

$$\alpha=\frac{\pi r_0^2\Lambda}{\sigma^2} \quad (7)$$

and

$$\beta=\frac{gf}{N_c}\frac{1}{\tau_s}\int_0^{\tau_s}\exp\left[-\frac{E_d}{kT(t)}\right]dt . \quad (8)$$

This represents a simple analytical expression to be easily compared with the experiments.

Figure 5 resports the experimental difference between the growth rate of the doped layers and that of undoped layers versus dopant concentration. Data, extracted from the results reported in Sec. II, are shown for B, P, and As. It is quite striking that for all of the three dopants the simple form of Eq. (6) is found to hold. In fact, Eq. (6) provides an excellent fit of the experimental data (solid lines). The fits were obtained using for β values of 9.7×10^{-19}, 3.4×10^{-20}, and 8×10^{-21} cm^{-3} for B, P, and As, respectively. Of course it is not possible to discriminate among the different parameters of Eq. (8). For instance, for P, considering a short spike at a constant temperature of 1700 K, one can choose $g=2$, $f=0.02$, and $E_d=-0.45$ eV. These are reasonable values, but equally good fits can be also obtained with different values. It is likely that the large difference in the rate enhancement produced by P or As and that produced by B can be accounted for by different values of the donor and acceptor level. The small difference between P and As should instead be attributed to different values in the activated fraction f.

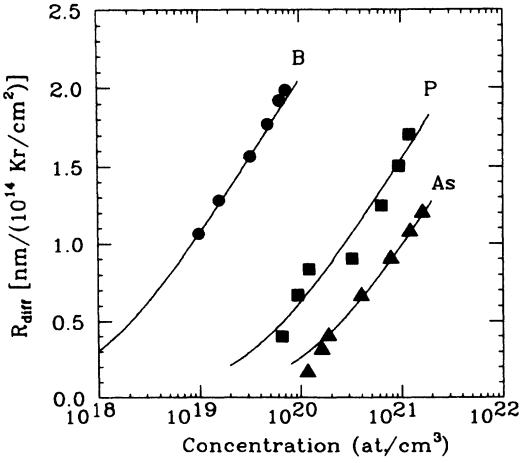

FIG. 5. Difference, $R_{\rm diff}$, between the ion-induced growth rate of doped a-Si layers and that of undoped layers as a function of dopant concentration. Experimental data are reported for B, P, and As and refer to irradiations with 600-keV Kr ions at 350°C. The solid lines are fits to the data.

Though the parameters cannot be exactly determined, the main issue is that the predicted functional form is apparently right. Moreover, the slope of all of the three curves is the same, as required by Eq. (6). This slope equals $\pi r_0^2 \Lambda/\sigma^2$. It should be noted that these are not fitting parameters since the ratio Λ/σ^2 has been taken directly from the Jackson model,[15] and r_0 can be chosen only in the small range of $\sim 3-10$ nm (we have used a value of 7.2 nm). This means that the experimental slope just came out to be that required by Eq. (6). We think this cannot be simply a coincidence.

A model in which the influence of dopants on the growth rate is mainly ascribed to the electrical properties predicts the presence of a compensating effect, i.e., silicon with equal amounts of *n*- and *p*-type doping should behave as an impurity-free material. A compensating effect in the growth rate has been indeed observed during pure thermal annealing.[26] During IBIEC, however, only a partial compensation is present.[6] Recent experiments[6] have shown that the ion-induced growth rate of an *a*-Si layer doped with both B and P at a constant concentration of $1\times10^{20}/\text{cm}^3$, though smaller than that of a simply B-doped layer, is still higher than that of intrinsic material. The occurrence of a partial compensation can still be understood within the presence intracascade description. In fact, only a region ~ 15 nm in diameter, surrounding the ion track, is involved in the thermal spike, and therefore in kink generation. The Fermi-level position is determined by the number of dopants which are present at the interface within this hot region. For instance, at a dopant concentration of $1\times10^{20}/\text{cm}^3$ the number of dopants present in this region is just ~ 10 atoms. This is indeed a small number. Therefore, a compensated sample contains, as an average, 10 B and 10 P atoms within this region. Of course fluctuations of these numbers become rather important and, in each collision cascade, the sample behaves sometimes as an *n*-type, sometimes as a *p*-type (depending whether P atoms are in excess over B atoms, or vice versa), and only rarely as an intrinsic material. Since both *n*- and *p*-type samples produce a rate enhancement, the final result is still an enhancement with respect to an impurity-free sample. This enhancement, however, is less pronounced than for a simply B-doped layer because a partial dopant compensation indeed occurs within each collision cascade. These observations qualitatively explain the presence of a partial compensation during IBIEC.

V. CONCLUSION

In conclusion, in the present work we have proposed a phenomenological description of ion-beam-induced epitaxial crystallization of *a*-Si. The model is based on the assumption that the same defect responsible for thermal annealing also produces IBIEC. Following the thermal description of recrystallization proposed by Williams and Elliman, we have identified this defect in a kinklike step which forms into [110] ledges at the {111} terraced *c-a* interface. These kinks are thought to be generated thermally within the thermal-spike regime of each collision cascade. Since kinks represent a structural deformation of the *c-a* interface, they do not exist away from the interface itself. This observation agrees well with the experimental results demonstrating that only those defects generated right at the *c-a* interface are responsible for IBIEC. Moreover, we have noted that kinks generate and annihilate in pairs. They therefore behave like the defects postulated in the Jackson model of IBIEC. Our approach assumed further that, after kink generation, their temporal evolution is completely described by the intracascade model proposed by Jackson. The structural and electronic properties of kinks have allowed us to quantitatively explain the orientation and doping dependences of IBIEC. In particular, the logarithmic relationship between the ion-induced growth rate and dopant concentration is completely understood.

We think that the present description, combining structural and electronic features of the thermal models with the nonequilibrium features of IBIEC models, provides a unifying, consistent interpretation of the crystallization phenomena, both in the thermal and in the ion-beam-induced regime. More experimental work is needed to further test the model.

ACKNOWLEDGMENTS

We thank S.U. Campisano for his stimulating interest throughout the different stages of this work. This work was supported in part by Progetto Finalizzato Materiali e Dispositivi per l'Elettronica a Stato Solido (MADESS), Consiglio Nazionale delle Richerche (CNR).

[1] I. Golecki, G. E. Chapman, S. S. Lau, B. Y. Tsaur, and J. W. Mayer, Phys. Lett. **71A**, 267 (1979).

[2] J. Nakata, M. Takahashi, and K. Kajiyama, Jpn. J. Appl. Phys. **20**, 2211 (1981).

[3] J. Linnros, B. Svensson, and G. Holmen, Phys. Rev. B **30**, 3629 (1984).

[4] J. Linnros, G. Holmen, and B. Svensson, Phys. Rev. B **32**, 2770 (1985).

[5] J. S. Williams, R. G. Elliman, W. L. Brown, and T. E. Seidel, Phys. Rev. Lett. **55**, 1482 (1985).

[6] F. Priolo, A. La Ferla, and E. Rimini, J. Mater. Res. **3**, 1212 (1988).

[7] J. M. Poate, J. Linnros, F. Priolo, D. C. Jacobson, J. L. Batstone, and M. O. Thompson, Phys. Rev. Lett. **60**, 1322 (1988).

[8] J. Linnros, R. G. Elliman, and W. L. Brown, J. Mater. Res. **3**, 1208 (1988).

[9] A. La Ferla, S. Cannavò, G. Ferla, S. U. Campisano, E. Rimini, and M. Servidori, Nucl. Instrum. Methods B **19/20**, 470 (1987).

[10] D. M. Maher, R. G. Elliman, J. Linnros, J. S. Williams, R. V. Knoell, and W. L. Brown, in *Materials Modification and Growth Using Ion Beams*, Vol. 93 of *Materials Research Society Symposium Proceedings*, edited by U. J. Gibson, A. E. White, and P. P. Pronko (MRS, Pittsburgh, 1987), p. 87.

[11] F. Priolo, C. Spinella, A. La Ferla, E. Rimini, and G. Ferla,

Appl. Surf. Sci. **43**, 178 (1989).
[12]See, e.g., G. L. Olson and J. A. Roth, Mater. Sci. Rep. **3**, 1 (1988), and references therein.
[13]H. A. Atwater, C. V. Thompson, and H. I. Smith, Phys. Rev. Lett. **60**, 112 (1988).
[14]H. A. Atwater, C. V. Thompson, and H. I. Smith, in *Fundamentals of Beam-Solid Interactions and Transient Thermal Processing,* Vol. 100 of *Materials Research Society Symposium Proceedings,* edited by M. J.Aziz, L. E. Rehn, and B. Stritzker (MRS, Pittsburgh, 1988), p. 345.
[15]K. A. Jackson, J. Mater. Res. **3**, 1218 (1988).
[16]J. Linnros, W. L. Brown, and R. G. Elliman, in *Fundamentals of Beam-Solid Interactions and Transient Thermal Processing,* Vol. 100 of *Materials Research Society Symposium Proceedings,* edited by M. J. Aziz, L. E. Rehn and B. Stritzker (MRS, Pittsburgh, 1988), p. 369.
[17]F. Spaepen and D. Turnbull, in *Laser Annealing of Semiconductors,* edited by J. M. Poate and J. W. Mayer (Academic, New York, 1982), p. 15.
[18]I. Suni, G. Goltz, M.-A. Nicolet, and S. S. Lau, Thin Solid Films **93**, 171 (1982).
[19]J. S. Williams and R. G. Elliman, Phys. Rev. Lett. **51**, 1069 (1983).
[20]G. L. Olson, S. A. Kokoroski, R. A. McFarlane, and L. D. Hess, Appl. Phys. Lett. **37**, 1019 (1980).
[21]T. Diaz de la Rubia, R. S. Averback, R. Benedek, and W. E. King, Phys. Rev. Lett. **59**, 1930 (1987).
[22]W. L. Johnson, Y. T. Cheng, M. Van Rossum, and M. A. Nicolet, Nucl. Instrum. Methods B **7/8**, 657 (1985).
[23]L. T. Chadderton, *Radiation Damage in Crystals* (Wiley, New York, 1965).
[24]A. Goldsmith, T. Waterman, and H. Hirschhorn, *Handbook of Thermophysical Properties of Solid Materials* (Macmillan, New York, 1961).
[25]T. Papa, F. Scudieri, M. Marinelli, U. Zammit, and G. Cembali, J. Phys. (Paris) **44**, Colloq. C5-73 (1983).
[26]I. Suni, G. Goltz, M. G. Grimaldi, M.-A. Nicolet, and S. S. Lau, Appl. Phys. Lett. **40**, 269 (1982).